Supporting Information

Two-dimensional High-entropy MWN_2 Nanosheets for Boosted Water Oxidation under Alkaline Media

Jiajing Wu[1, #], Shida Bao[2, #], Shan Jiang[3], Qiting Shao[2], Xuexia Lan[4], Tao Zhang[4], Xiao Yan[1], Zhi Yang[5], Chengliang Chai[5], Zhijun Dong[1], Zheng-Jie Chen[2*] and Jing Peng[2*]

[1]Institute of Information Technology, Shenzhen Institute of Information Technology, Shenzhen, 518172, China.

[2]Faculty of Materials Science and Energy Engineering, Shenzhen University of Advanced Technology, Shenzhen, 518107, China.

[3]The 710 Research Institute of CSSC, Yichang 443000, China

[4]Low dimensional Energy Materials Research Center, Institute of Technology for Carbon Neutrality, Shenzhen Institutes of Advanced Technology, Chinese Academy of Sciences, Shenzhen, 518055, China.

[5]The fifth engineering co., LTD of China Railway Seventh Group, Zhengzhou, 450009, China.

[#]These authors contributed equally to this work and should be considered co-first authors.

*Corresponding Authors: Zheng-Jie Chen, Jing Peng

*E-mail: zj.chen2@siat.ac.cn; jing.peng@siat.ac.cn

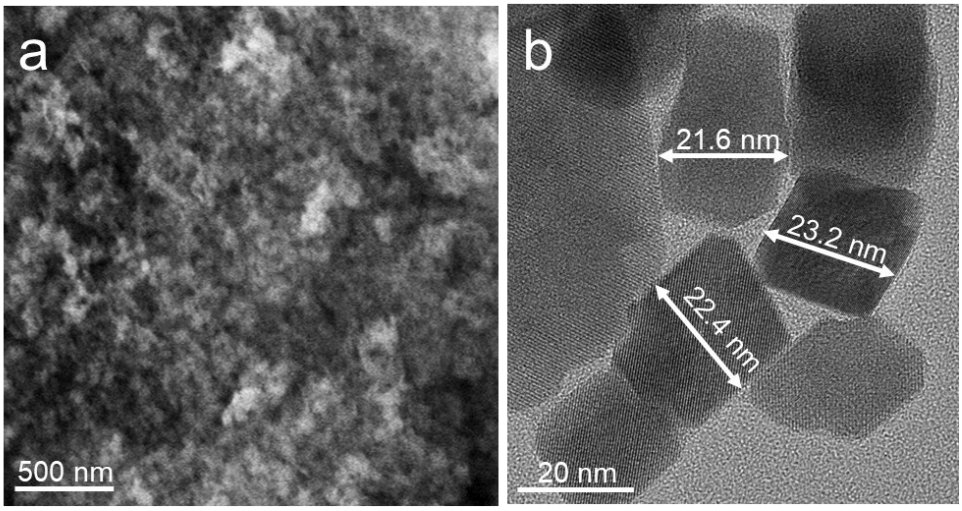

Figure S1. a) SEM image and b) TEM image of tungsten oxide precursor prepared in hydrothermal method with an average size of the sample particles of approximately 22 nm.

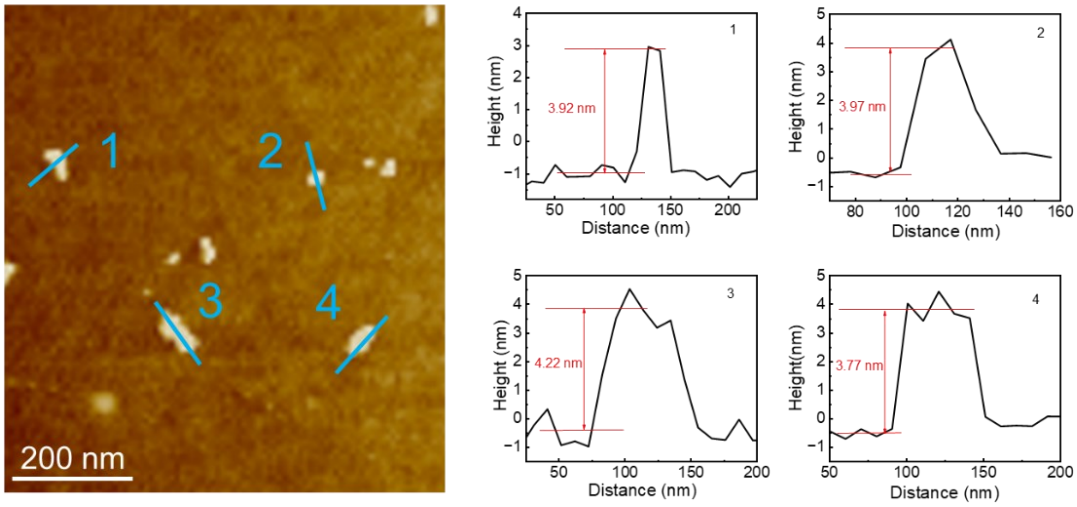

Figure S2. AFM image of (FeCoNiMn)WN_2 nanosheets.

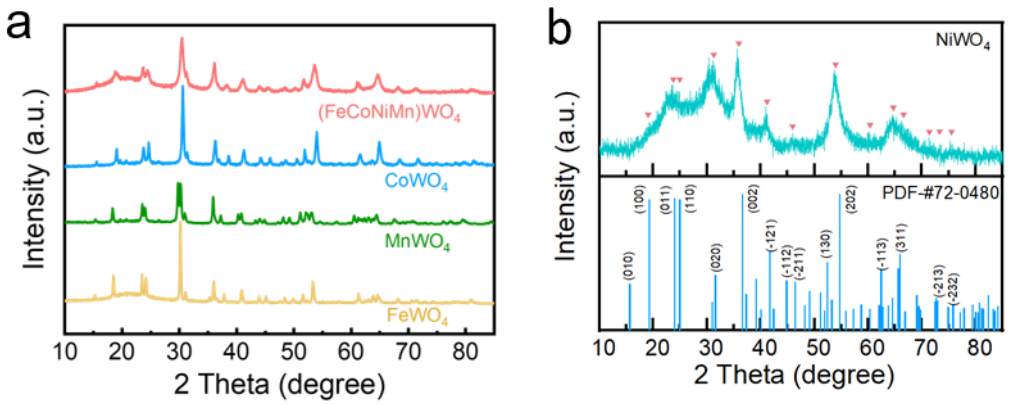

Figure S3. XRD patterns of different samples. XRD patterns of a) tungsten oxide precursors. b) $NiWO_4$.

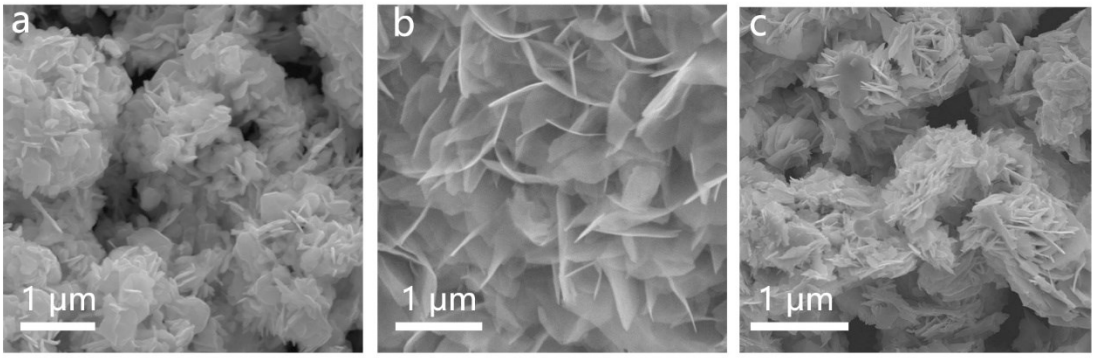

Figure S4. SEM image of MWN_2 nanosheet. a) $FeWN_2$. b) $CoWN_2$. c) $MnWN_2$.

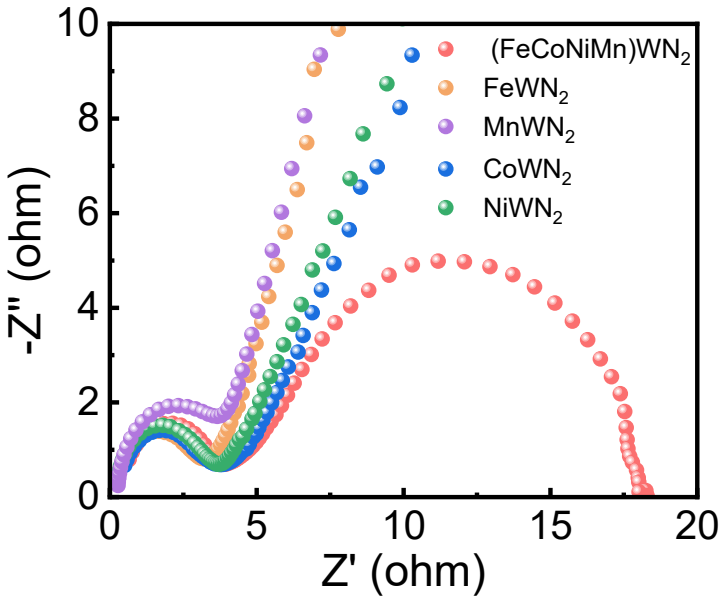

Figure S5. EIS results of the electrocatalysts measured at 0.6 V (vs. RHE) with an amplitude over the frequency range from 100 kHz to 0.1 Hz.

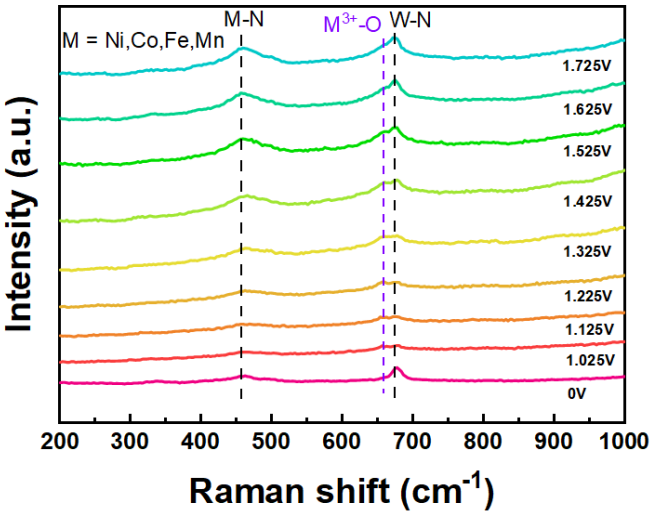

Figure S6. Raman spectra of $FeCoNiMnWN_2$ nanosheets.

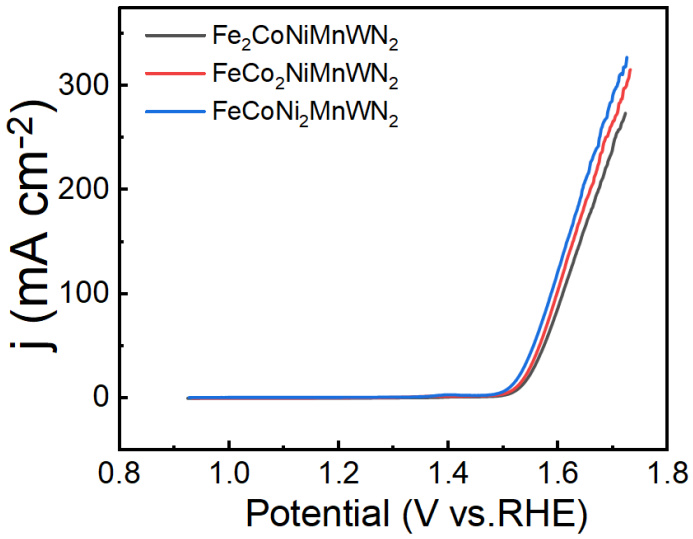

Figure S7. LSV of M(FeCoNi)$MnWN_2$ nanosheets with different ratios components.

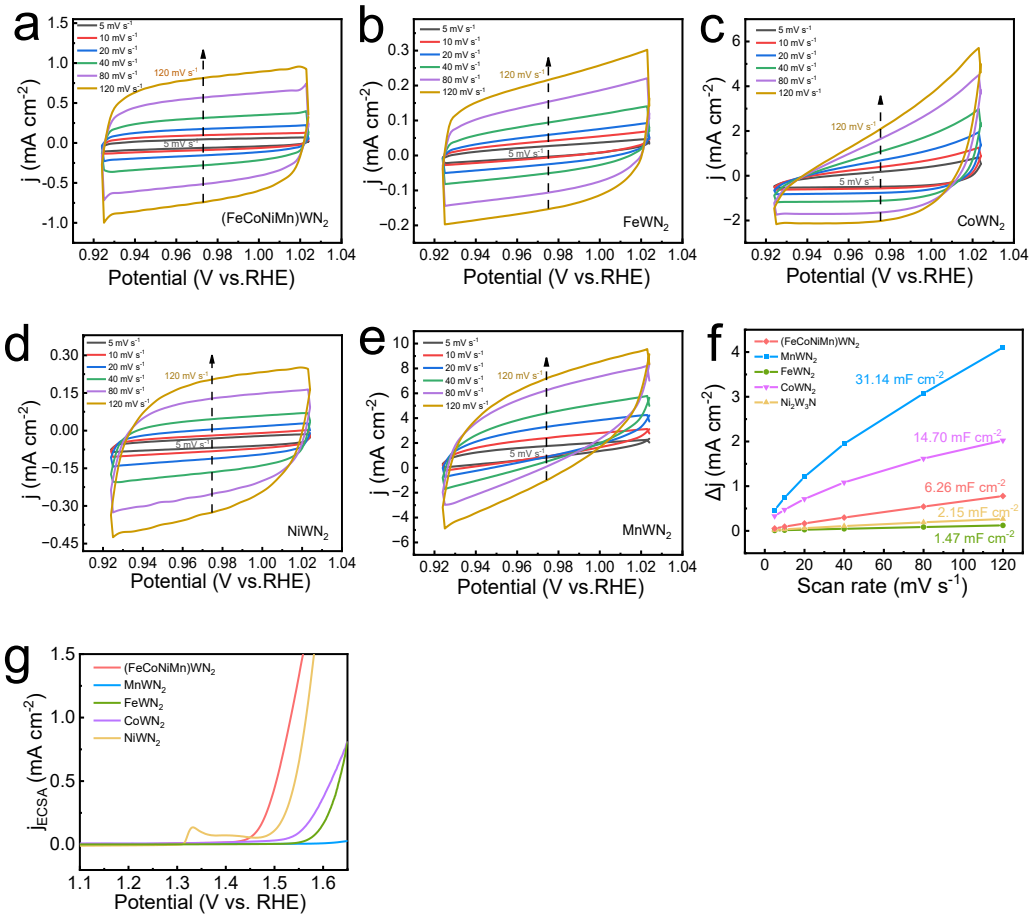

Figure S8. C_{dl} for different electrocatalysts and the corresponding ECSA. CV cycling tests in 0.924-1.024 (V vs. RHE) voltage range with sweep rates (5, 10, 20, 40, 80, 120 mV s^{-1}) of a) $(FeCoNiMn)WN_2$. b) $FeWN_2$. c) $CoWN_2$. d) $NiWN_2$. e) $MnWN_2$. f) Scan rate was plotted as a function of the corresponding current density. g) The normalized electrocatalytic performance of ECSA.

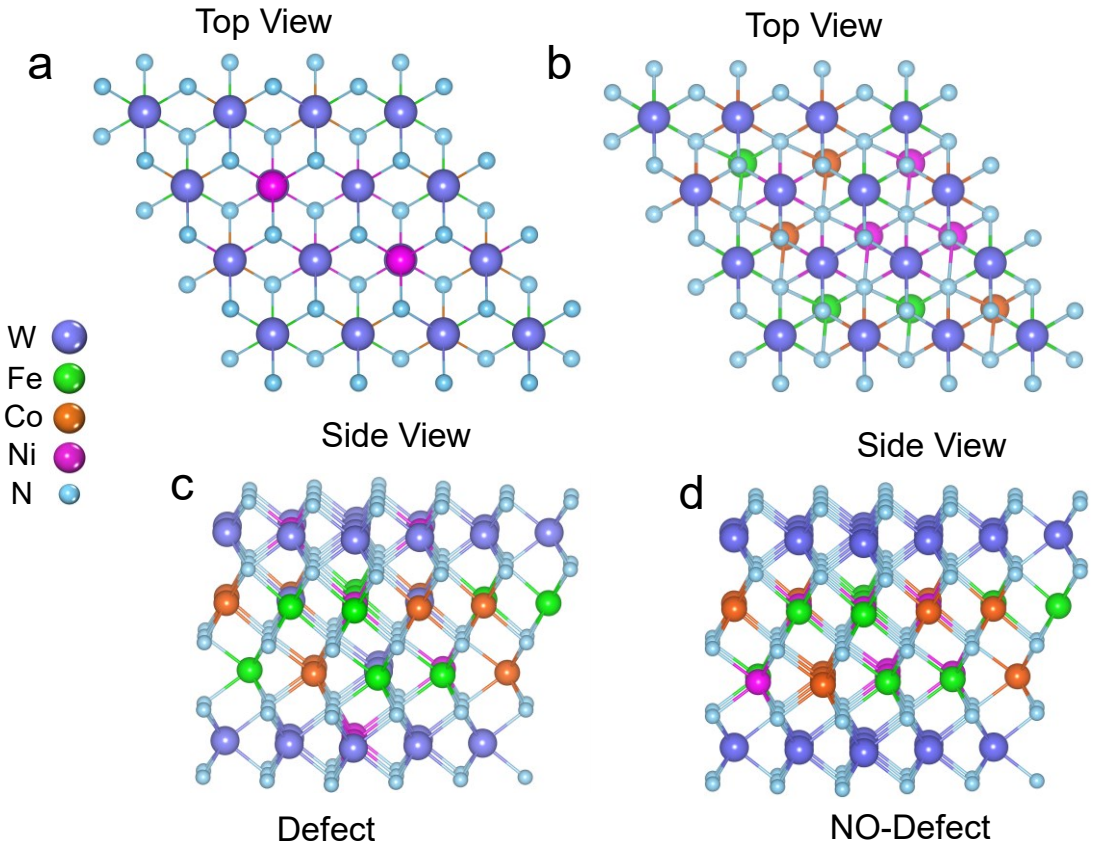

Figure S9. Models of Ni-antisite and W-site. a-b) Top view structure for Ni-antisite and W-site. c-d) Side view structure for Ni-antisite and W-site.

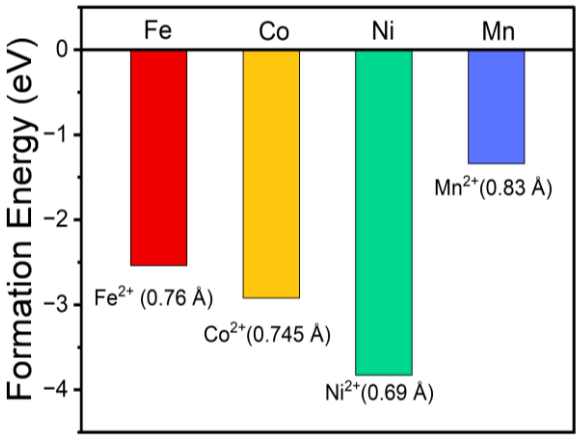

Figure S10. Defect formation energies of different M-W combinations and their relationship with ionic radii.

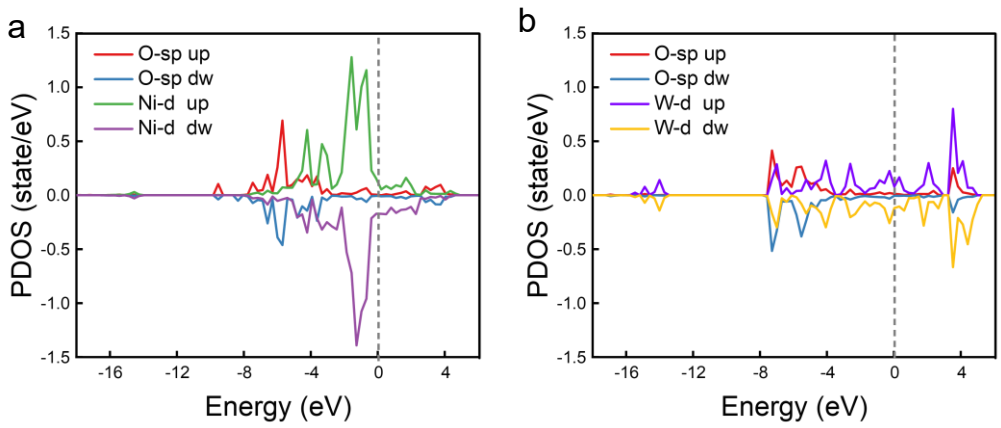

Figure S11. PDOS of a) Ni-antisite and b) W-site.

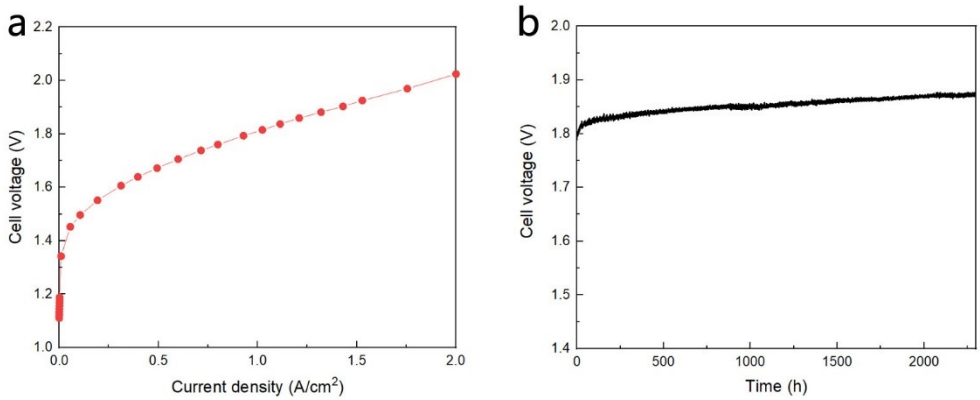

Figure S12. The performance of alkaline water electrolysis for the cell of (-) Pt/C || (FeCoNiMn)WN_2 (+) at 60℃. a) Polarization curve. b) Long-term stability test at 1A/cm^2.

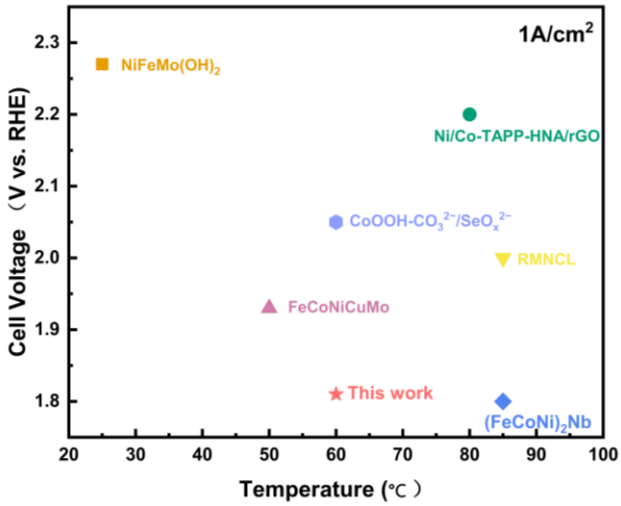

Figure R13. Comparison of the performance of materials reported in other literature.

Table S1. Ratio of different elements measured by XPS.

Name	C1s	N1s	O1s	Fe2p	Co2p	Ni2p	Mn2p	W4f
Atomic %	42.58	12.18	23.77	2.53	2.41	2.39	5.42	8.72

Table S2. Comparison of the performance of materials reported in other literature.

Catalyst	Temperature(℃)	Potential (V vs. RHE)	Reference
$FeCoNiMnWN_2$	60	1.81@1A/cm^2	This work
FeCoNiCuMo	50	1.93@1A/cm^2	[1]
$(FeCoNi)_2$ Nb	85	1.80@1A/cm^2	[2]
Ni/Co-TAPP-HNA/rGO	80	2.20@1A/cm^2	[3]
RMNCL	85	2.00@1A/cm^2	[4]
$NiFeMo(OH)_2$	25	2.27@1A/cm^2	[5]
$CoOOH\text{-}CO_3^{2-}/SeO_x^{2-}$	60	2.05@1A/cm^2	[6]

[1] P.-S. Jhu, C.-W. Chang, C.-C. Cheng, Y.-C. Ting, T.-Y. Lin, F.-Y. Yen, P.-W. Chen, S.-Y. Lu, Nano Energy **2024**, 126, 109703.

[2] Z. Li, R. Wu, D. Duan, X. Liu, R. Li, J. Wang, H. Chen, S.-W. Chen, Y. Wu, H. Wang, S. Jiang, X. Zhang, Z. Lu, Joule **2024**, 8, 2920–2937.

[3] K. Wei, Z. Liu, G. Feng, Y. Wang, S. Zhang, X. Li, M. Zhang, H. Li, J. Zhou, S. Lei, F. Gao, Advanced Energy Materials **2025**, 2405366.

[4] W. Ma, Y. Zhang, B. Wang, J. Wang, Y. Dai, L. Hu, X. Lv, J. Dang, Chemical Engineering Journal **2024**, 494, 153212.

[5] J. Wang, Z. Xing, R. Kang, Y. Zheng, Z. Zhang, T. Ma, Y. Wang, B. Yin, Y. Liao, L. Li, C. Cheng, S. Li, Advanced Functional Materials **2024**, 2418439.

[6] J. Zhao, Z. Xue, Q. Wang, X. Li, S. Liu, X. Zhao, Journal of Energy Chemistry 2024, 97, 46–54.